

## Janus Emulsions for the Detection of Bacteria

Qifan Zhang,<sup>†</sup> Suchol Savagatrup,<sup>†</sup> Paulina Kaplonek,<sup>‡,§</sup> Peter H. Seeberger,<sup>\*,‡,§</sup>  
and Timothy M. Swager<sup>\*,†,§</sup>

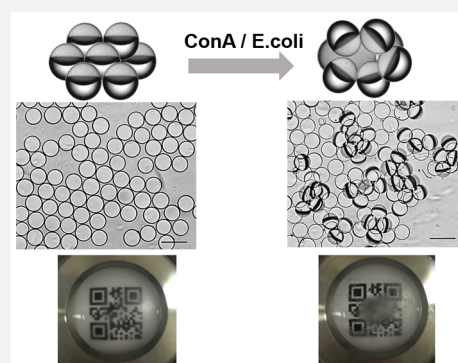
<sup>†</sup>Department of Chemistry and Institute for Soldier Nanotechnologies, Massachusetts Institute of Technology, 77 Massachusetts Avenue, Cambridge, Massachusetts 02139, United States

<sup>‡</sup>Department of Biomolecular Systems, Max Planck Institute of Colloids and Interfaces, Am Mühlenberg 1, 14476 Potsdam, Germany

<sup>§</sup>Institute of Chemistry and Biochemistry, Free University Berlin, Arnimallee 22, 14195 Berlin, Germany

### Supporting Information

**ABSTRACT:** Janus emulsion assays that rely on carbohydrate–lectin binding for the detection of *Escherichia coli* bacteria are described. Surfactants containing mannose are self-assembled at the surface of Janus droplets to produce particles with lectin binding sites. Janus droplets orient in a vertical direction as a result of the difference in densities between the hydrocarbon and fluorocarbon solvents. Binding of lectin to mannose(s) causes agglutination and a tilted geometry. The distinct optical difference between naturally aligned and agglutinated Janus droplets produces signals that can be detected quantitatively. The Janus emulsion assay sensitively and selectively binds to *E. coli* at  $10^4$  cfu/mL and can be easily prepared with long-time stability. It provides the basis for the development of inexpensive portable devices for fast, on-site pathogen detection.



Foodborne pathogens are a growing global public health concern. An estimated 73,000 illnesses and 60 deaths occur annually in the United States alone as a result of consuming pathogen contaminated food and water.<sup>1</sup> *Escherichia coli*, for example, can be easily spread in contaminated food and water to cause serious illness and even death. In a serious 1996 *E. coli* outbreak in Japan, more than 6,000 primary schoolchildren became sick and at least 12 died;<sup>2</sup> while in Canada, seven of the thousands of people that fell ill died in 2000.<sup>3</sup> Such tragedies could have been avoided if inexpensive and fast devices to test large amounts of food and water for pathogenic bacteria prior to consumption were available. The conventional method for bacterial detection requires cell culturing and a multiday enrichment step.<sup>4</sup> Modern methods based on surface plasmon resonance (SPR),<sup>5</sup> the polymerase chain reaction (PCR),<sup>6,7</sup> and immunoassays<sup>8</sup> are much more rapid but require expensive equipment that has to be operated by trained technicians. These drawbacks of the current methods surrender the possibility of food testing before consumption. As a result, an on-site detection method that is rapid, inexpensive, and user-friendly is urgently needed.

We report an emulsion based agglutination assay for the selective and sensitive detection of bacteria. Fluid Janus droplets are powerful liquid phase sensing particles when the different hemispheres are functionalized to have orthogonal physical and biochemical properties. Janus particles with covalently modified surfaces have been used for sensing applications.<sup>9,10</sup> We produce liquid Janus emulsions with intrinsic functionalization by using surfactant-based recognition groups. Liquid Janus emulsions provide dynamic and compliant

surfaces that mimic properties of live cells. We have targeted carbohydrate–lectin interactions that are critical to cellular recognition,<sup>11</sup> and utilize many weak interactions in a multivalent binding process.<sup>12</sup> Although a commercial agglutination assay (latex fixation assay) has been used for identifying bacteria, it involves the functionalization of latex beads with expensive antigen or antibody and counting agglutination sites under a microscope.<sup>13</sup> Our emulsion assay uses the carbohydrate surfactant molecule, which self-assembles at the droplet surfaces during the emulsification process so that no further functionalization is required for bacteria recognition. Additionally, the intrinsic optical lensing behavior of the Janus droplets also enables both qualitative and quantitative detection of protein and *E. coli* bacteria. Surfactants lower the interfacial tension between two immiscible liquids and stabilize emulsion droplets. Recently, we demonstrated that stimulus-responsive surfactants can produce dynamic complex emulsions that undergo morphological switching.<sup>14</sup> This mechanism depends on changes in concentration or effectiveness of the surfactants and hence requires many chemical reactions to change a single droplet. In this study, we report a more sensitive transduction mechanism that does not require changes in the interfacial tensions, but rather uses the changes in the alignment of the Janus droplets for the detection of analytes. Janus morphology was maintained during the binding process, and the analyte is directly visualized by the tilted Janus droplets.

Received: January 14, 2017

Published: March 23, 2017

Initially, we investigated the interactions between the Janus droplets and a mannose-binding lectin, concanavalin A (ConA), which serves as a functional substitute for *E. coli* bacteria.<sup>15</sup> A simple mannose carrying an anomeric C-14 alkyl chain (ManC14) was designed as the surfactant and was synthesized via a modified literature method.<sup>16</sup> Janus emulsions, composed of equal volumes of hexane and FC770 (a commercially available perfluorinated solvent from 3M) in aqueous continuous phase, were fabricated. Both monodispersed and polydispersed droplets were used in this study. The detailed fabrication procedure and the dynamic nature of these droplets are explained in the [Supporting Information](#). ManC14 and Zonyl FS300, a commercially available fluorocarbon surfactant, were then used to stabilize the emulsion assay in the Janus morphology. The Janus emulsion assay can be prepared in large scale while maintaining the stability and sensing behavior over several months. The force of gravity aligned the denser FC-770 phase downward, leading to the spontaneous alignment of the Janus emulsions in an upright direction with the hydrocarbon phase and ManC14 on top ([Figure 1a](#)). Aligned Janus

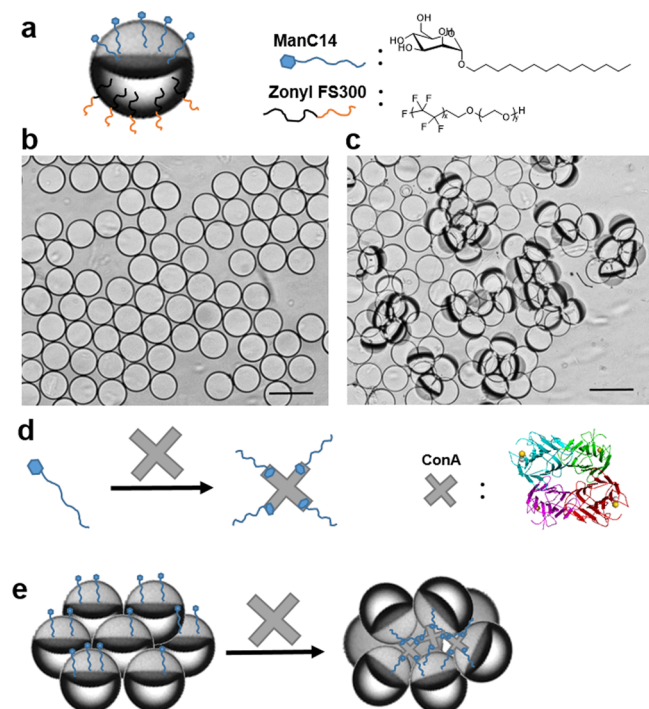


**Figure 1.** (a) Side view of a Janus droplet stabilized by ManC14 and Zonyl FS 300. (b, c) Optical micrographs of (b) transparent pristine monodispersed Janus emulsions and (c) agglutinated Janus emulsions scattering light after exposure to ConA. Scale bar 100  $\mu\text{m}$ . (d, e) Schematic representation of Janus emulsion agglutination: (d) multivalent binding of ConA to ManC14; (e) agglutinated Janus emulsions with ConA and ManC14.

emulsions appeared as transparent simple droplets under the microscope, and the internal structure was not apparent ([Figure 1b](#)). However, upon the addition of a buffered solution of ConA and gentle agitation, bound Janus droplets realigned in a unique tilted configuration with the hexane faces joined together in an agglutinated configuration ([Figure 1c](#)) within seconds. The hydrocarbon surfactant ManC14 self-assembled at the hexane/water interface to lower the interfacial tension and created an affinity for ConA on the hydrocarbon

hemisphere. ConA has four mannose binding subunits ([Figure 1d](#)) and cross-links the droplets via the hydrocarbon phase to generate the tilted (agglutinated) clusters ([Figure 1e](#)).

Janus emulsions can become H/F/W double emulsions when additional fluorocarbon surfactant is added. To confirm that the hexane phases of Janus droplets were connected via ConA, excess fluorocarbon surfactant Zonyl was added to the agglutinated emulsion assay to induce a morphology change from Janus to double emulsions. Under these conditions, nonagglutinated Janus emulsions transform symmetrically into double emulsions H/F/W ([Figure 2a,c](#)). However, with ConA-

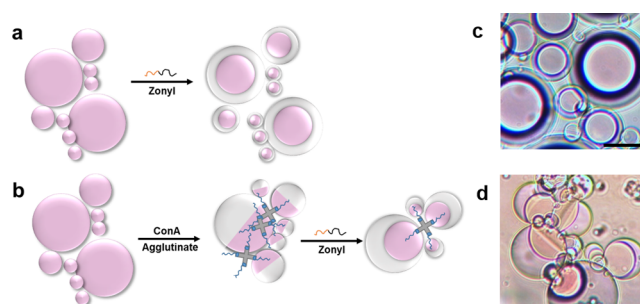


**Figure 2.** Scheme and optical images showing directional morphology change with addition of excess Zonyl surfactant. The hexane phase has been dyed in pink for display purposes. (a, c) Janus emulsion change into H/F/W double emulsion. (b, d) Agglutinated Janus emulsion with addition of ConA. Scale bar equals 50  $\mu\text{m}$ .

agglutinated Janus emulsions, the droplets maintained an asymmetric structure wherein the preorganized ConA:ManC14 groups behaved as a persistent connective anchor to the hydrocarbon phase ([Figure 2b,d](#) and see also a video in the [Supporting Information](#)). Bovin serum albumin (BSA) was used as a non-mannose binding protein for the control experiments. No agglutination or significant perturbation of the optical properties was observed with even high concentration of BSA (up to 1 mg/mL, see the [Supporting Information](#)).

Janus emulsions with the chosen fluids have compensating refractive indices which enable detection by optical transmission. Vertically aligned droplets on a horizontal surface are transparent, whereas the agglutinated droplets are highly scattering. (Refractive indices of fluids: hexane, 1.37; FC770, 1.27; water, 1.33. Ratio of water/FC770 = 1.05  $\approx$  hexane/water = 1.03, thus resulting in no scattering when light is transmitted through a vertically aligned Janus droplet.) This significant change can be easily observed by visual detection without any instrumentation or energy. Beyond a qualitative scattering/nonscattering assay, quantitative detection schemes are possible when image processing algorithms are employed to analyze the optical micrographs.

In an effort to create a qualitative binary assay for analytes, Janus emulsions were placed in a transparent analysis chamber that was positioned over a quick response (QR) code printed on paper ([Figure 3a](#)). Upon the addition of ConA, the Janus droplets agglutinated and the chamber became opaque, rendering the QR code unreadable by a smartphone ([Figure 3b](#)). This change occurred within less than five seconds after the addition of ConA and gentle agitation, which enables the Janus emulsion assay for a detection with instant readout. The Janus droplets behave as lens, and the optical scattering is strongest at distances  $>5$  mm. At shorter distances, the QR

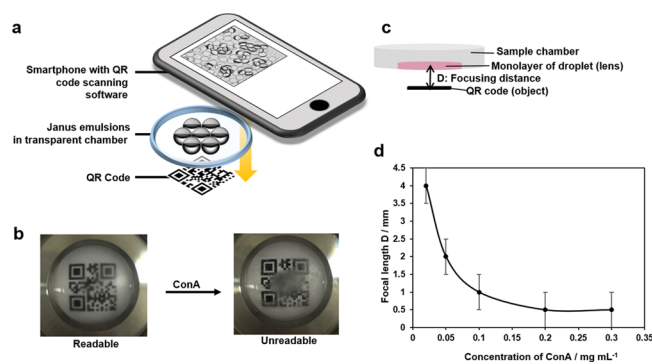


**Figure 3.** (a) Schematic view of qualitative detection of the agglutinated Janus emulsions. The Janus emulsions are placed on a transparent analysis chamber. The QR code enables the binary qualitative detection of agglutination. (b) Optical signal detected using a QR code before and after exposure to ConA. (c) The focusing distance  $D$ , with droplet monolayer as a lens and QR code as the object. (d) Correlation of the threshold ConA concentration for the binary signal with  $D$ .

code can still be scanned and the distance ( $D$ ) at which the code was readable varies with ConA concentration (Figure 3c). The greater the  $D$ , the lower the concentration of ConA required to disable the QR code. As a result, binary distance dependent measurements can provide some level of quantitation.

To precisely quantify the degree of agglutination, we implemented an image processing program to calculate the percentage of area covered by agglutinated Janus emulsions by evaluating the differences in optical intensity of the images before and after exposure to ConA. The program uses the adaptive thresholding algorithm to distinguish areas with higher transparency (pristine Janus emulsions) from the opaque regions (agglutinated Janus emulsions) (see Supporting Information). Optical micrographs of Janus emulsions, Figure 4a–c, show that the opaque regions increase with higher

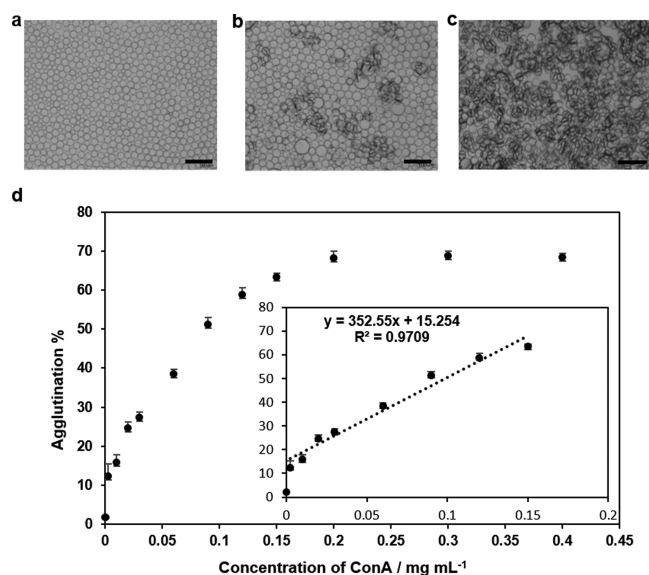


**Figure 4.** Correlation of ConA concentration and agglutination level: (a) Janus emulsion without ConA; (b) with  $0.03 \text{ mg mL}^{-1}$  ConA; (c) with  $0.12 \text{ mg mL}^{-1}$  ConA. (d) Correlation between ConA concentration and agglutination level. Scale bar equals  $250 \mu\text{m}$ .

concentration of ConA. The agglutination level was defined by the percentage of areas covered by agglutinated (scattering) Janus droplets (Figure 4d). Each point represents an average of multiple pictures ( $N \geq 5$ ) obtained at the given concentration of ConA. The background without addition of ConA (Figure 4a) was analyzed with the software and showed nearly zero agglutination level output. We observed a linear correlation between agglutination level and the concentration of ConA up to  $150 \mu\text{g mL}^{-1}$  (Figure 4d). At higher concentrations of ConA, agglutinated droplets saturated the imaging area, and thus a plateau in the agglutination percentage was observed.

Having established a detection scheme with the help of ConA, bacterial detection of *E. coli* ORN 178 strains was explored. These bacteria express the mannose-specific lectin, FimH, for the recognition and binding to host cells. Agglutination of droplets was observed 48 h after incubation with live *E. coli*. Unexpectedly, a change in morphology from Janus to H/F/W double emulsions was observed in addition to agglutination (Figure 5a). Symmetric Janus droplets are

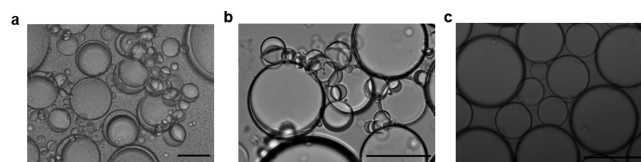


**Figure 5.** Micrographs showing emulsion agglutination with *E. coli* bacteria. (a) Janus emulsions change into H/F/W double emulsion after 48 h incubation with live ORN 178 *E. coli*. Agglutination is also observed. (b) Janus emulsion agglutination, 2 h after 4% paraformaldehyde treated ORN 178 *E. coli* bacteria ( $10^4 \text{ cfu/mL}$ ) were added. (c) No agglutination was observed with ORN 208 strains under the same testing conditions. Scale bar equals  $100 \mu\text{m}$ .

produced when the ManC14 and Zonyl concentrations are adjusted such that hexane/water and FC770/water interfacial tensions are equal. When live *E. coli* binds to ManC14, the cell appears to either reduce the effectiveness of ManC14 as surfactant at the interface or, perhaps more likely, remove some ManC14 from the droplets. The active ManC14 that was present on the surface of droplets may have been significantly decreased due to the high concentration of bacteria ( $>10^9 \text{ cfu/mL}$ ) after 48 h of proliferation. In this case, the Zonyl stabilized FC770/water interface had a lower interfacial tension resulting in the equilibrium morphology of the double emulsion (H/F/W). This morphological change was not observed upon the addition of ConA since the lectin itself is small and inanimate, and neither decreases the effectiveness of ManC14 nor removes it from the droplet. We speculate that the slower rate of agglutination for the emulsions with live bacteria as compared to ConA resulted from the dynamic nature of the pili that contain the FimH recognition elements.<sup>17</sup>

To accelerate agglutination, bacteria were fixed via 4% paraformaldehyde.<sup>18</sup> While maintaining the FimH binding activity, the fixed pili are static,<sup>19</sup> similar to ConA, and are more efficient in agglutinating droplets. Janus emulsion agglutination was observed after 2 h with paraformaldehyde treated ORN 178 strains. To determine the limit of detection, treated bacteria were diluted to various concentrations and agglutination was detected using a smartphone and QR code recognition for ORN 178 strains at  $10^4 \text{ cfu/mL}$  (see the Supporting Information for a movie on smartphone-based *E. coli* detection). It is important to note that this method is



comparable in sensitivity to the existing methods for pathogen detection. The conventional plating technique can detect single bacteria, but the culturing process takes several days. Other immunological and bioluminescence methods as well as the nucleic acid based assays have a detection limit of  $10^3$ – $10^4$  cfu/mL, but require special laboratory equipment and trained technicians.<sup>20</sup>

As a control, ORN 208 strains, carrying a mutation in the FimH gene that compromises the pili's ability to bind mannose, were subjected to the same tests, and no agglutination was observed at the concentrations that suffice to detect ORN 178 (Figure 5b, Figure 5c). Similar to the agglutination assay with ConA, agglutination was observed and the Janus morphology was maintained. A transformation to a double emulsion at these lower concentrations of fixed bacteria was not observed. We expect that this system can be further improved by employing more elaborate carbohydrate surfactants. In a real-world application, customized protocols will be necessary for sample preparation, and there may be interfering effects. To address the latter we have conducted investigations with non-mannose binding protein and find that the binding is not affected by the generic protein (Figure S4).

In summary, we have developed a Janus emulsion agglutination assay based on carbohydrate–lectin binding. The mannose surfactant functionalized emulsion assay described in this work was designed specifically for *E. coli* as a model system. The assays can be expanded to arrays with multiple carbohydrate surfactants to differentiate various types of bacterial strains. The self-assembly of glycosylated surfactant molecules on the surface of droplets provided multivalent binding sites to target analytes. We demonstrated that this agglutination detection method can be analyzed qualitatively with a QR code for a binary readout and quantitatively with designed image processing software. Both methods give results within a minute. The Janus emulsion assay allows for the detection of *E. coli* bacteria at a concentration of  $10^4$  cfu/mL. Therefore, this method is comparable in sensitivity to the existing methods for pathogen detection. The Janus emulsion agglutination assay is a fast, inexpensive, and sensitive method that can be implemented with commercial smartphones for on-site detection of biomolecules and pathogens.

## ■ ASSOCIATED CONTENT

### Supporting Information

The Supporting Information is available free of charge on the ACS Publications website at DOI: 10.1021/acscentsci.7b00021.

Detailed methods and instrumentation, synthetic procedures, Janus emulsion assay preparation, bulk emulsification for polydispersed Janus emulsion, generation of monodispersed Janus emulsions via microfluidics, and details on ConA sensing and *E. coli* sensing (PDF)  
Morphological change without agglutination (MPG)  
Morphological change with agglutination (MPG)  
*E. coli* sensing (MPG)

## ■ AUTHOR INFORMATION

### Corresponding Authors

\*E-mail: Peter.Seeberger@mpikg.mpg.de.

\*E-mail: tswager@mit.edu.

### ORCID

Timothy M. Swager: 0000-0002-3577-0510

## Notes

The authors declare the following competing financial interest(s): MIT has filed for a patent on the detection method and compositions described in this publication.

## ■ ACKNOWLEDGMENTS

We are grateful for support from the Abdul Latif Jameel World Water and Food Security Lab at the Massachusetts Institute of Technology, the Army Research Office through the Institute for Soldier Nanotechnologies at the Massachusetts Institute of Technology. Q.Z. thanks the Legatum Center for Development and Entrepreneurship at the Massachusetts Institute of Technology. T.M.S. is appreciative of the support of the Alexander von Humboldt Foundation. P.H.S. gratefully acknowledges generous financial support by the Max Planck Society and by the DFG (SFB-TR 84).

## ■ ABBREVIATIONS

*E. coli*, *Escherichia coli*; ConA, concanavalin A; QR code, quick respond code; cfu, colony-forming unit

## ■ REFERENCES

- (1) Frenzen, P. D.; Drake, A.; Angulo, F. J.; The Emerging Infections Program Foodnet Working Group. Economic Cost of Illness due to *Escherichia Coli* O157 Infections in the United States. *J. Food Prot.* **2005**, *68* (12), 2623–2630.
- (2) Watanabe, Y.; Ozasa, K.; Mermin, J. H.; Griffin, P. M.; Masuda, K.; Imashuku, S.; Sawada, T. Factory Outbreak of *Escherichia Coli* O157:H7 Infection in Japan. *Emerging Infect. Dis.* **1999**, *5* (3), 424–428.
- (3) O'Connor, D. R. *Part One: A Summary Report of The Walkerton Inquiry*; Ontario Ministry of the Attorney General Press: Ontario, 2002; pp 1–35.
- (4) Doyle, M. P.; Buchanan, R. L. *Food Microbiology: Fundamentals and Frontiers*, 4th ed.; American Society for Microbiology Press: Washington, DC, 2012.
- (5) Bhunia, A. K. Biosensors and Bio-Based Methods for the Separation and Detection of Foodborne Pathogens. *Adv. Food Nutr. Res.* **2008**, *54*, 1–44.
- (6) McKillip, J. L.; Jaykus, L.-A.; Drake, M. Influence of Growth in a Food Medium on the Detection of *Escherichia Coli* O157: H7 by Polymerase Chain Reaction. *J. Food Prot.* **2002**, *65* (11), 1775–1779.
- (7) Nakano, S.; Kobayashi, T.; Funabiki, K.; Matsumura, A.; Nagao, Y.; Yamada, T. PCR Detection of *Bacillus* and *Staphylococcus* in Various Foods. *J. Food Prot.* **2004**, *67* (6), 1271–1277.
- (8) Notermans, S.; Wernars, K. Immunological Methods for Detection of Foodborne Pathogens and Their Toxins. *Int. J. Food Microbiol.* **1991**, *12* (1), 91–102.
- (9) Yoshida, M.; Roh, K. H.; Mandal, S.; Bhaskar, S.; Lim, D.; Nandivada, H.; Deng, X.; Lahann, J. Structurally Controlled Bio-Hybrid Materials Based on Unidirectional Association of Anisotropic Microparticles with Human Endothelial Cells. *Adv. Mater.* **2009**, *21* (48), 4920–4925.
- (10) Suci, P. A.; Kang, S.; Young, M.; Douglas, T. A Streptavidin-Protein Cage Janus Particle for Polarized Targeting and Modular Functionalization. *J. Am. Chem. Soc.* **2009**, *131* (26), 9164–9165.
- (11) Lis, H.; Sharon, N. Lectins: Carbohydrate-Specific Proteins That Mediate Cellular Recognition. *Chem. Rev.* **1998**, *98* (2), 637–674.
- (12) Grünstein, D.; Maglinao, M.; Kikkeri, R.; Collot, M.; Barylyuk, K.; Lepenies, B.; Kamena, F.; Zenobi, R.; Seeberger, P. H. Hexameric Supramolecular Scaffold Orients Carbohydrates to Sense Bacteria. *J. Am. Chem. Soc.* **2011**, *133*, 13957–13966.
- (13) Weinberg, G. A.; Storch, G. A. Preparation of Urine Samples for Use in Commercial Latex Agglutination Tests for Bacterial Antigens. *J. Clin. Microbiol.* **1985**, *21* (6), 899–901.

- (14) Zarzar, L. D.; Sresht, V.; Sletten, E. M.; Kalow, J. a.; Blankschtein, D.; Swager, T. M. Dynamically Reconfigurable Complex Emulsions via Tunable Interfacial Tensions. *Nature* **2015**, *518* (7540), 520–524.
- (15) Huang, C. C.; Chen, C. T.; Shiang, Y. C.; Lin, Z. H.; Chang, H. T. Synthesis of Fluorescent Carbohydrate-Protected Au Nanodots for Detection of Concanavalin A and Escherichia Coli. *Anal. Chem.* **2009**, *81* (3), 875–882.
- (16) Adasch, V.; Hoffmann, B.; Milius, W.; Platz, G.; Voss, G. Preparation of Alkyl  $\alpha$ - and  $\beta$ -D-Glucopyranosides, Thermotropic Properties and X-Ray Analysis. *Carbohydr. Res.* **1998**, *314* (3–4), 177–187.
- (17) Thanassi, D. G.; Bliska, J. B.; Christie, P. J. Surface Organelles Assembled by Secretion Systems of Gram-Negative Bacteria: Diversity in Structure and Function. *FEMS Microbiol. Rev.* **2012**, *36* (6), 1046–1082.
- (18) Chao, Y.; Zhang, T. Optimization of Fixation Methods for Observation of Bacterial Cell Morphology and Surface Ultrastructures by Atomic Force Microscopy. *Appl. Microbiol. Biotechnol.* **2011**, *92* (2), 381–392.
- (19) Yago, T.; Leppänen, A.; Carlyon, J. A.; Akkoyunlu, M.; Karmakar, S.; Fikrig, E.; Cummings, R. D.; McEver, R. P. Structurally Distinct Requirements for Binding of P-selectin Glycoprotein Ligand-1 and Sialyl Lewis x to *Anaplasma phagocytophilum* and P-selectin. *J. Biol. Chem.* **2003**, *278* (39), 37987.
- (20) Mandal, P. K.; Biswas, A. K.; Choi, K.; Pal, U. K. Methods for Rapid Detection of Foodborne Pathogens: An Overview. *Am. J. Food Technol.* **2011**, *6* (2), 87–102.